# Performance of a reversible heat pump / organic Rankine cycle unit coupled with a passive house to get a Positive Energy building

Dumont, Olivier; Do Carmo, Carolina Madeira Ramos; Fontaine, Valentin; Randaxhe, Francois; Quoilin, Sylvain; Lemort, Vincent; Elmegaard, Brian; Nielsen, Mads Pagh

*Published in:*
Journal of Building Performance Simulation

*DOI (link to publication from Publisher):*
10.1080/19401493.2016.1265010

*Publication date:*
2018

*Document Version*
Accepted author manuscript, peer reviewed version

# Performance of a inversible heat pump / organic Rankine cycle unit coupled with a passive house to get a Positive Energy Building

Olivier Dumont, Carolina Carmo, Valentin Fontaine, François Randaxhe, Sylvain Quoilin, Vincent Lemort, Brian Elmegaard, Mads P. Nielsen

*Olivier Dumont, Thermodynamics and Energetics Laboratory, Chemin des chevreuils, 7 B49, 4000 Liege (Belgium), Olivier.dumont@ulg.ac.be, 0032498/226404 or 00324 366 48 27*

*Carolina Carmo, Department of Energy Technology, Aalborg University, Aalborg, Denmark, cca@et.aau.dk, 004541770147*

*Valentin Fontaine, valentin.fontaine@student.ulg.ac.be, Thermodynamics and Energetics Laboratory, Chemin des chevreuils, 7 B49, 4000 Liege (Belgium), 0493504243*

*Francois Randaxhe, Thermodynamics and Energetics Laboratory, Chemin des chevreuils, 7 B49, 4000 Liege (Belgium), F.Randaxhe@ulg.ac.be, 0032 495 41 12 69*

*Sylvain Quoilin, Thermodynamics and Energetics Laboratory, Chemin des chevreuils, 7 B49, 4000 Liege (Belgium), squoilin@ulg.ac.be, 00324 366 48 22*

*Vincent Lemort, Thermodynamics and Energetics Laboratory, Chemin des chevreuils, 7 B49, 4000 Liege (Belgium), Vincent.Lemort@ulg.ac.be, 00324 366 48 01*

*Brian Elmegaard, Department of Mechanical Engineering, DTU, Lungby, Denmark, be@mek.dtu.dk , 0045 45254169*

*Mads P. Nielsen, Department of Energy Technology, Aalborg University, Aalborg , Denmark, mpn@et.aau.dk , 0045 99409259*

*This work was supported and funded by the Eurostars Program (Single HPA Unit).*

# Performance of a inversible heat pump / organic Rankine cycle unit coupled with a passive house to get a Positive Energy Building

## Abstract

This paper presents an innovative technology that can be used to deliver more renewable electricity production than the total electrical consumption of a building while covering the heat demand on a yearly basis. The technology concept uses a heat pump (HP), slightly modified to revert its cycle and generate electricity, coupled to a solar thermal collector roof. This reversible HP/organic Rankine cycle unit presents three operating modes: direct heating, HP and organic Rankine cycle. This work focuses on describing the dynamic model of the multi-component system followed by a techno-economic analysis of the system under different operational conditions. Sensitivity studies include: building envelope, climate, appliances, lighting and heat demand profiles. It is concluded that the HP/ORC unit can turn a single-family house into a PEB under certain weather conditions (electrical production of 3012 kWh/year and total electrical consumption of 2318 kWh/year) with a 138.8 $m^2$ solar roof in Denmark.

## Keywords

Heat Pump, Organic Rankine cycle, Positive Energy Building, Dynamic Simulation, Annual Performance

## Nomenclature

| | |
|---|---|
| A | Area [$m^2$] |
| B | Income benefits [€] |
| COP | Coefficient of performance [-] |
| $c_p$ | Specific heat capacity at constant pressure [J/(kgK)] |
| e | Empirical variable used in the roof model [-] |
| f | Factor [-] |
| i | Index [-] |
| I | Irradiance [$W.m^{-2}$] |
| M | Mass [kg] |
| N | Number of plates [-] |
| P | Cost [$€.W^{-1}h^{-1}$] |
| $\dot{Q}$ | Heat transfer [W] |
| r | Interest rate [%] |
| s | Empirical constant [-] |
| t | Time [s] |
| T | Temperature [°C] |
| U | Heat transfer coefficient [$W.m^{-2}.K^{-1}$] |
| v | Empirical constant used in the roof model[-] |
| W | Energy [W.h] |
| $\dot{W}$ | Power [W] |

| | |
|---|---|
| x | Empirical constant [-] |
| y | Empirical constant [-] |
| z | Empirical constant [-] |
| | |
| Ω | Numeric coefficient [-] |
| η | Efficiency [-] |
| β | Collector tilt [°] |
| Δ | Difference [-] |
| γ | Cover factor [-] |
| ζ | Emittance [-] |
| Ρ | Density [kg/m$^3$] |
| | |
| CHP | Combined Heat and Power |
| DH | Direct heating |
| DHW | Domestic Hot Water |
| FH | Floor Heating |
| GHX | Horizontal ground heat exchanger |
| HP | Heat pump |
| HP/ORC | Inversible HP/ORC unit |
| HP/PV | HP combined with PV |
| NZEB | Net Zero Energy Building |
| ORC | Organic Rankine Cycle |
| PEB | Positive Energy Building |
| PV | Photovoltaic panels |
| amb | Ambient |
| b | Back |
| bb | Buy-back |
| BH | Borehole |
| cons | Consumption |
| D | Demand |
| ex | Exhaust |
| FH (floor) | Floor heating |
| HGHE | Horizontal ground heat exchanger |
| h | High |
| in | Indoor |
| l | Low |
| l-a | Lightning and appliances |
| m | Mean |
| match | matching |
| min | Minimum |

| | |
|---|---|
| net | Net |
| p | Plate |
| prod | Production |
| O | Overall |
| out | Outdoor |
| r | Retail |
| roof | Solar roof |
| S | Supply |
| sto | Storage |
| su | Supply |
| T | Top |

# 1. Introduction

### *1.1 Context*

By 2020, greenhouse gases emissions must be reduced by 20% as compared to the levels of 1990, according to European objectives (20-20-20 objectives) (European Commission 2011). This goal should be achieved through an increase in the proportion of renewable energy sources from 9% to 20% together with a 20% increase in system energy efficiency. Households account for 27% of the final energy consumption (European Commission 2011) and therefore can constitute an important part of the solution. Various technologies and concepts are being investigated, developed and implemented in the building sector. Net Zero Energy Buildings (Marszal et al. 2010) are expected to gain a significant importance: by 2019, all new buildings in the European Union should present a renewable energy production higher than their primary energy consumption (European commission 2010).
Net Zero Energy Buildings and, by extension, Positive Energy Buildings (PEB) will therefore play a major role in the future.  Positive Energy Buildings offer different advantages: relatively high independence from energy prices, lower long-term running costs and zero fuel consumption among others. Amongst the different available energy sources, solar energy is pointed as a very interesting choice for PEB because it is free, 100% renewable and available in abundance.

### *1.2 Concept – the inversible heat pump / organic Rankine cycle unit*

In this paper, the concept of coupling a inversible heat pump / organic Rankine cycle unit to a passive house to get a PEB is investigated (Figure 1). A HP/ORC inversible unit is a heat pump which is slightly modified to be able to work as an organic Rankine cycle (ORC). This inversible unit coupled to a passive house, a large solar thermal roof and a horizontal ground heat exchanger constitutes a combined system able to provide electricity and heat to the household. There are three operating modes: the direct heating (DH) mode uses the heat produced by the roof to collect the thermal energy in a water store which supplies the floor heating (FH) and Domestic Hot Water (DHW). In case of unfavorable meteorological conditions, the heat pump mode (HP) allows to heat the thermal energy store efficiently. Finally, a large quantity of heat is generated on the roof during mid-season and summer periods. This surplus heat can be converted into electricity by means of the ORC (Dumont et al. 2015a).

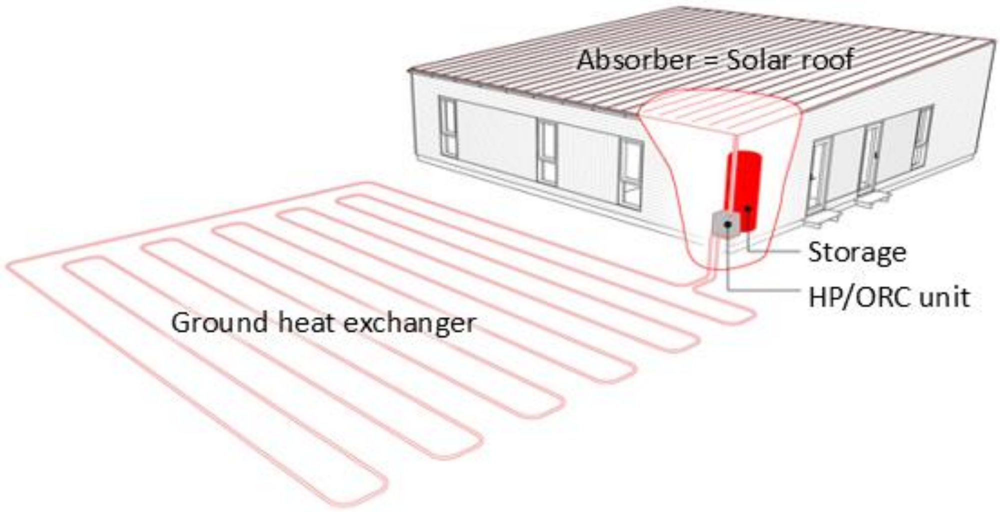


Figure 1: The inversible HP/ORC unit integrated in the house (Dumont et al. 2015a).

The first investigation on such a system has been introduced in 2011 (Schimpf et al. 2011). A thermo-economical tool was developed but only a small area of collector (12 m2) and a vertical ground heat exchanger was considered. In 2013, the modelling and sizing of such a unit has been investigated. The optimal sizing based on an existing house in Denmark (300m long horizontal ground heat exchanger, 500 liters heat storage and 138.8 m2 solar roof) lead to a 5 kWe ORC system (Quoilin et al. 2013, 2015).
The theoretical results were promising with an ORC electrical production seven times higher than the electrical heat pump annual consumption. A prototype has therefore been built and successfully tested (Dumont et al. 2014a; Dumont et al. 2015a). A cycle efficiency of 4.2% was achieved in ORC mode (with condensation and evaporation temperature respectively of 25 °C and 88 °C) and a COP of 3.1 was obtained in HP mode (with condensation and evaporation temperature respectively of 61 °C and 21 °C).

### *1.3 Scope*

The first part of this paper details the models of: theinversible HP/ORC unit ,the passive house ,the horizontal ground heat exchanger and the flat plate solar roof collector. Each sub-model, the global model and the control strategy of the system are described in detail in section 2.
The model is then used to simulate and assess the energy system performance in typical days along the year for this innovative concept (Section 3). Followed by a study of influence including building envelope, location, heat demand, lighting and appliances profiles is performed based on annual results (section 4)
Finally, an economic comparison with a heat pump and photovoltaic panels, is made.

## 2. Modeling

### *2.1 Simulation tool*

Among simulation programs, some are dedicated to building performance simulation (IDA ICE, ESP-r, EnergyPlus, TRNSYS, WUFI®Plus…) while others are more general (Dymola/Modelica, MATLAB/ Simulink, IDA SE…). Simulation tools like Matlab–Simulink need the model to be implemented, in a state-space form in which causal relations play an important role. A simulation language based on an object oriented approach and physically oriented connections – Modelica - is chosen as simulation tool to model the new system proposed in this work. Recently, Modelica has become more and more used in building performance simulation. The Lawrence Berkeley National Laboratory developed a Modelica library called Buildings that contains a large number of HVAC components and a multi-zone building model (Wetter, Zuo and Nouidui 2011). Also, the RWTH Aachen and UdK Berlin (Nytsch-Geusen and Unger 2009) are developing Modelica libraries for HVAC-systems and building models . Besides, many models for HVAC components and different thermal zone models, the RWTH Aachen library offers a database of manufacturer's data for building technology (Muiller and Badakhshani 2010).

Before describing each sub-model and the control strategy, it is important to note that the dynamic modeling of a system including several sub-systems does not systematically require each model to be dynamic: components characterized by relatively low time constants can be modelled as quasi-steady-state, since their fast dynamics are not relevant to the overall simulation and can substantially impact the computational effort. In this case, it was shown previously (Perers, 1997, Chow, 1993, Schnieders, 1997, Fischer et al 2004, Dumont et al 2014a and Freeman et al, 2015) that the dynamics of the inversible unit can be neglected because of its small inertia compared to other sub-systems.

### *2.2 Reversible HP/ORC unit*

An experimental investigation has been carried out on the unit in HP and ORC mode over a wide range of conditions (Dumont et al 2015a). Based on the measurements, semi-empirical models have been calibrated for each component (heat exchangers, compressor, pump and pipes). These models are then combined to simulate the behavior of the global system. Finally, polynomial regressions, fitted on the global validated model, allow to evaluate the outputs of the inversible unit. These are presented by the authors in a former paper (Dumont et al. 2014a).

### *2.3 Storage*

The basic type of hot water storage tank in the HP/ORC system is shown in Figure A1. It is a typical domestic hot water tank system installed in single-family houses in Denmark (500 liters). The water tank consists of a stainless steel cilinder with two built-in spiral heat exchangers (HXs) – one going from mid-height to bottom of the tank and another going from bottom to the top of the tank. The working fluid in the HP/ORC unit is circulated through the mid-height helical heat exchanger, while the cold water from the grid is circulated through the all-through heat exchanger to supply DHW. In the current work, this stratified sensible thermal storage is modeled by a one-dimensionl finite-volume method comprising 20 isothermal segments with equal volume (Carmo et al, 2015). The model accounts for heat losses to the environment, internal heat conduction between adjacent cells as well as for internal natural convection whenever an internal reversed temperature gradient occurs. The dynamic temperature profile of the tank is represented by a set of *i* ordinary differential equations that represent the energy balance of the tank (Equation (1)). The first term is the thermal inertia of the cell.
The second term is composed (from left to right) of the enthalpy flow, the thermal exchange with an eventual heat exchanger, conduction with adjacent cells and ambient losses.

$$A_i \Delta x \rho_i c_p \frac{dT_i}{dt} = \dot{m}\left(h_{ex.i} - h_{su,i}\right) + A_{hx.i}\dot{Q}_{hx} + \alpha A_{i+1}\dot{Q}_{i+1} + \Omega A_{i-1}\dot{Q}_{i-1} - A_{amb}U(T_i - T_{amb}) \quad (1)$$

In this equation α is 0 if the *i* th node is the top of the tank and 1 otherwise and β is 0 if the

*i* th node is the bottom node and 1 otherwise. This model is validated using experimental data under different charging and discharging conditions following prEN12977-3:2008 (CEN 2008).
More details can be found in a former work (Carmo et al. 2015).

### *2.4 Solar roof*

The solar roof currently installed in the house is a prototype of aluminum pipes installed on an aluminum absorber plate covered with the Alanod Miorosol coating (Innogie Aps 2013). A four milimeter thick glass surface is added to ensure the glazing (Figure A2). Commonly, thermal panels are smaller, but in this case it is more interesting to cover the whole roof (138.8 m$^2$) because the excess heat in summer is not wasted and can be converted into electricity trough the ORC. This large roof size is classical for new buildings in the countryside of Denmark.

The heat collected by the roof is therefore modeled with Equation (2) involving the useful solar roof area ($A$), the outdoor temperature ($T_{amb}$), the mean absorber temperature ($T_m$), the overall heat transfer coefficient ($U_o$) and the solar irradiance absorbed by a collector per unit area of absorber ($I$).

$$\dot{Q}_{roof} = A(I - U_o(T_m - T_{amb})) \qquad 2$$

The overall heat transfer coefficient ($U_o$) is the sum of the top loss coefficient ($U_T$), the edge loss coefficient ($U_E$) and the back loss coefficient ($U_b$). The edge loss coefficient is assumed to be zero, since the heat trasnfer is negligible when the collector area is higher than 30 m$^2$ (Duffie and Beckmam 2006). The back loss coefficient is also assumed to be zero due to the 400 mm thick insulation at the back of the collector. Finally, the top loss coefficient is evaluated using Eq. 3 with a maximum error of 0.3 W/m$^2$ for mean absorber temperatures below 200°C (Klein 1975).

$$U_T = \left( \frac{1}{\frac{v}{T_m}\left(\frac{T_m - T_a}{N + f}\right)^e} + \frac{1}{h_w} \right)^{-1} + \frac{\sigma(T_m + T_a)(T_m^2 + T_a^2)}{\frac{1}{\varepsilon_p + s.N.h_w} + \frac{2N + n - 1 + z.\varepsilon_p}{\varepsilon_g} - N} \qquad 3$$

The different terms composing Equation (3) are detailed in Appendices - Table A1. The dynamic model of the solar roof finally obtained by combining equation 1 with a thermal inertia corresponding to 104.6 liters of 30% volume glycol based water solution.

### *2.5 Building model*

The model is based directly on the geometry and the construction characteristics of the real Danish building. A simplified lumped parametric model is applied. The root mean squared error of a such a model related to inner temperature has been shown to be always lower than 1K (Masy 2007). The arrangement of the different rooms of the building and the composition of the walls are taken into account. The building is first divided into 5 zones (dinning room and kitchen, main bedroom, bathroom, hall and toilet and finally guest bedrooms. See zones characteristics in Figure A3 and table A2) with constant volume, uniform temperature and conservation of mass and energy in each zone. The walls are modeled with two thermal resistances and one heat capacity, parameters being given in Masy (2007). Four inputs are added in each zone: lighting, appliances, occupancy and a thermal exchange with adjacent zones. Wind pressure and buoyancy from the air specific volume difference and ventilation are not modeled in order to avoid too high level of complexity and computational time. Finally the radiant slab (25 $m^2$) from the buildings library (Wetter et al 2013) is connected to the only room where it exchanges heat in the house (zone 1).

### *2.6 Ground source horizontal heat exchanger (GHX)*

*Description of the case study*

The ground source horizontal heat exchanger consists of three layers layout. The layers are linked in parallel and buried respectively at 0.50, 1.00 and 1.50 meters depth. Each layer consists of 24 tubes disposed in a head to tail setting. The tubes are made in cross-linked polyethylene and are 22.89 m long with a diameter of 2.6 cm (Figure A4). 30% monoethylene glycol is used as heat transfer fluid. The soil is assumed to be argillaceous with a water content of 10%, which corresponds to an average soil humidity (Bircher, et al. 2012).

*Description of the model*

The deep earth temperature is set to 10 °C.This choice is made following ground measurements conducted in Potsdam, Germany, (PICIR 2015). The absorbance and emissivity of the soil surface are respectively set to 0.55 and 0.75. An average wind speed of 4 $m.s^{-1}$ is considered.

A model of the ground source horizontal heat exchanger already exists (using the finite element method) under the TRNSYS simulation language (TESS 2015). A reduced order model is developed and calibrated based on the reference finite element model (TESS 2015). This model is designed to be flexible and is valid for different kinds of pipes geometry and layout.

The model consists in discretizing three layers of ground (Figure 2). The central element in the model is the soil central thermal mass which simulates the soil directly surrounding the GHX pipes. In addition, a surface layer which reacts rapidly to climate variations (solar irradiation, ambient temperature and sky temperature) is added. Finally, a sub-soil layer presenting slow variations through the seasons is modeled and connected to the deep earth temperature.  Each layer is modeled with a  central capacity and two resistors The pipes are modeled with a finite volume 1D flow model (20 cells) from the Thermocycle library (Quoilin et al 2014). Finally, two thermal resistors are added to the pipes to account for the resistance of the tube and, for the latter, the resistance of the soil.

*Calibration of the reduced order model*

The reduced order model described here above is calibrated with the finite element model as a reference by variation of the two main inputs, which are the ambient temperature and the solar irradiation. The GHX model parameters are defined in Figura A6 (in the appendix). With these parameters, results show good agreement between the two models. A maximum deviation of 0.5 K is observed for the prediction of the water outlet temperature (Figure A5).

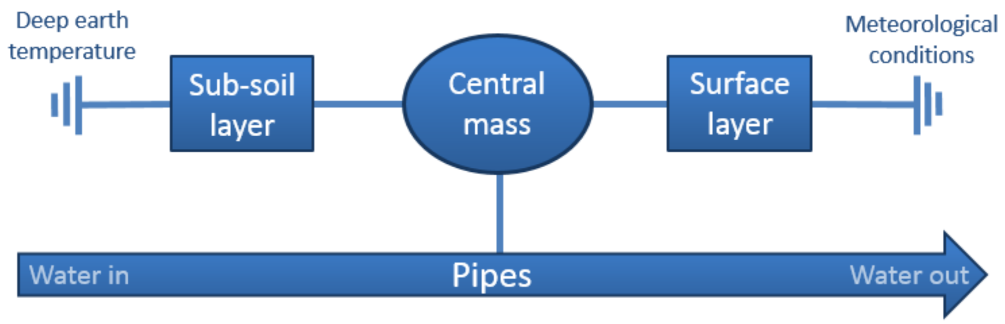


Figure 2: Layout of the reduced order model of the horizontal ground heat exchanger

### *2.7 Global model*

Figure 3 presents the flowchart of the global model combining the storage, the building, the roof, the inversible unit and the ground heat exchanger. Hourly schedules are associated to the occupancy, the domestic hot water use, the lighting and appliances in each zone (Georges et al. 2013). The weather data used for the outdoor temperature and the solar irradiance are provided by the DMI - Danish Meteorological Institute- (Wang et al. 2010) in the case of Denmark and by Energy Plus Energy Simulation Software (EnergyPlus 2015) for other locations. An adaptive time step is computed by the solver, but is not allowed to exceed 900 s. A low timestep induces too much computational time and too large output file size, a timestep larger than 20 minutes could lead to errors larger than 5% (Bouvenot et al 2015). The typical computational time is 3 hours for an annual simulation. The consumption of auxiliary pumps (except GHX pump) are neglected, they represent less than 2% of the global system power consumption.

Some parameters have to be fixed: Roof water flow rate, ground heat exchanger water flow rate, and storage water flow rate and temperature set points of the storage. Practically, the following values are used for the flow rates based on real values imposed in the house:

- Roof water flow rate = 0.6 $kg.s^{-1}$,
- Ground heat exchanger water flow rate = 1.5 $kg.s^{-1}$,
- Storage water flow rate = 0.6 $kg.s^{-1}$

These flow rates should be optimized in future investigations to increase the energy efficiency of the system (Burhenne et al 2013).

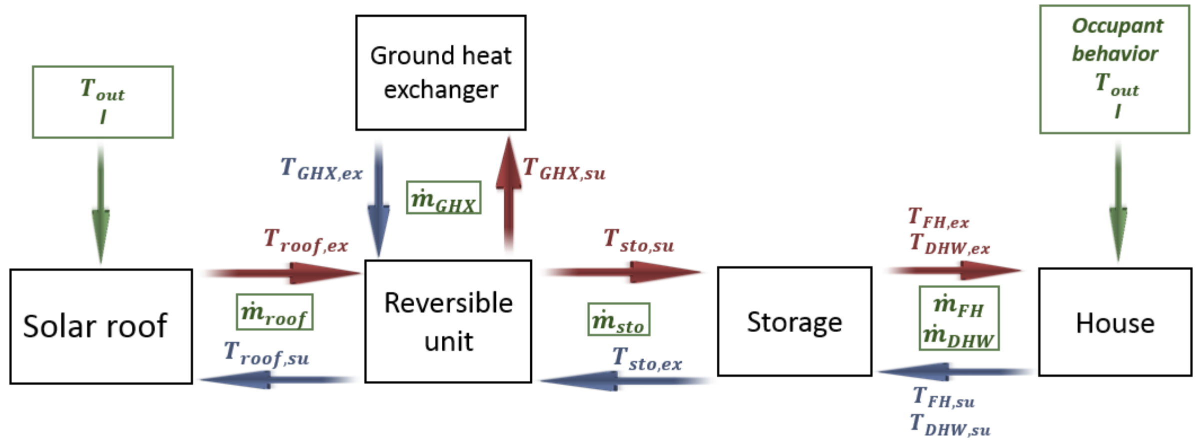


Figure 3: Global model and connections between sub-models.

### *2.8 Control*

The control strategy  ensures that the heat demand is covered while electricity is produced with the surplus of heat. For this reason the first control variable used is the hot water storage tank temperature (the control temperature point is located at mid-height of the tank).
A state diagram control is implemented. The conditions governing the transitions between the three modes (HP, ORC and DH) and the stand-by mode (Bypass) are shown in Figure 4. The Bypass mode means that no HP, ORC or DH is activated, only the floor heating circuit can be activated extracting energy from the water store, if necessary, to reach the desired indoor conditions (20°C). The principle is the following: if the storage is too cold (the control temperature of the storage is lower than the low-temperature threshold), the HP mode is activated. If the roof temperature is higher than the storage one, the DH mode is used. Finally, the ORC system produces electricity when the storage temperature has reached a given high threshold and if a stable state can be reached. This means that the ORC is only activated once it can produce a certain level of power ($W_{ORC}$,min). The  $W_{ORC,min}$ is used to enable a smooth and efficient operation of the system in ORC mode. When a stable operation of the ORC cannot be guaranteed ($W_{ORC}$ < $W_{ORC}$,min ),  the TES is allowed to go above the high temperature threshold. It should be noted that the HP mode, is using either the roof or the horizontal ground heat exchanger depending on which one is the warmest.

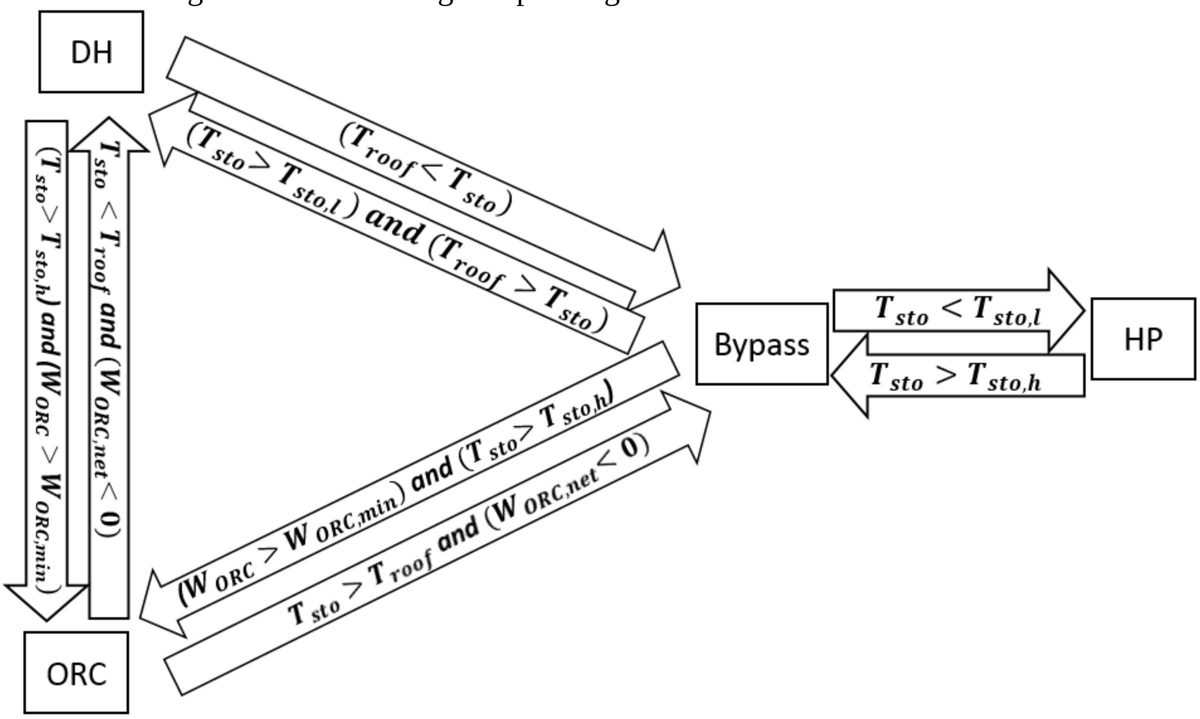


Figure 4: State diagram control. $T_{roof}$ is the roof exhaust temperature, $T_{sto}$ is the storage control temperature (middle height of the tank), $T_{sto,l}$ is the low temperature threshold of the storage, $T_{sto,h}$ is the high temperature threshold of the storage, $W_{ORC,min}$ is the minimum power to start the ORC system.

Table 1 summarizes the values of each threshold temperature. The threshold values were chosen to avoid chattering (too many mode changes) and to maximize the efficiency of the system in (Dumont et al. 2014a). The number of mode changes is considered high when more than one change occurs in a 15 minutes period.

Table 1: Values of the temperature thresholds

| Temperature threshold | Abbreviation | Value |
| --- | --- | --- |
| High temperature threshold of the storage | $T_{sto,h}$ [°C] | 50 |
| Low temperature threshold of the storage | $T_{sto,l}$ [°C] | 40 |
| Power threshold of the ORC | $W_{ORC,min}$ [W] | 2000 |
| Indoor comfort temperature | $T_{in}$ [°C] | 20 |

It should be noted that, although the set points and thresholds have been optimized, the proposed control strategy is still a myopic rule-based control strategy. A truly optimal control strategy is difficult to implement because of the high number of manipulated variables, the numerous set-points and the non-linearity of the problem. It would require a predictive non-linear optimization, based on the next 24 hours of weather forecast, user behavior and electricity prices. Such approach would avoid, for example, starting the heat pump when the solar heat will be sufficient to cover the heat demand later in the day.

## 3. Simulation of typical days

The system response is presented for three characteristic days in Denmark: a winter day (day 1), a spring day (day 62) and a summer day (day 182). Eight variables are analyzed in this section: the storage control temperature ($T_{sto}$), the outdoor temperature ($T_{out}$), the house ambient temperature in zone 1 ($T_{in}$), the exhaust roof temperature ($T_{roof}$), the ground heat exchanger exhaust temperature ($T_{GHX}$), the heat flow rate for floor heating ($\dot{Q}_{FH}$), the heat flow rate for Domestic Hot Water ($\dot{Q}_{DHW}$), the heat flow rate from the inversible unit ($\dot{Q}_{th,prod}$) and the electrical unit power consumption (-)/production (+) ($\dot{W}_{el}$).

### *3.1 Winter - Day 1*

The behavior of the system is plotted in Figure 5 for a characteristic winter day. Slightly after 1 a.m., the floor heating is activated ($\dot{Q}_{FH}$) in a way to keep the indoor temperature ($T_{in}$) close to 20°C. This leads to a decrease of the control temperature of the storage ($T_{sto}$) down to the lower temperature threshold of 40°C. The heat pump mode is therefore activated to raise the control temperature of the storage up to the high temperature threshold of the storage (50°C). This phenomenon is observed three times during this day (1 a.m., 11 a.m. and 5 p.m.). The heat generated in HP mode is $\dot{Q}_{HP/ORC}$ and corresponds to an electrical power of $\dot{W}_{el}$ in Figure 5. The direct heating mode cannot be activated because of the low temperature of the water in the roof ($T_{roof}$). In this case, the system is acting as a classical ground source heat pump during this typical winter day.

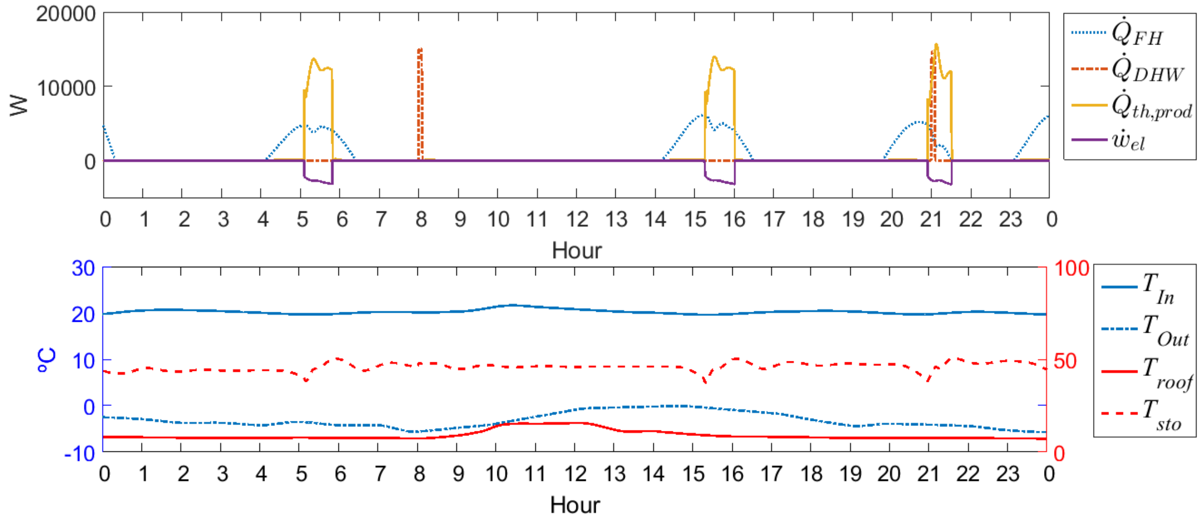


Figure 5: Dynamic simulation of the inversible unit coupled to a passive house for the 1st day of the year.

### *3.2 Spring - Day 62*

A typical spring day is depicted in

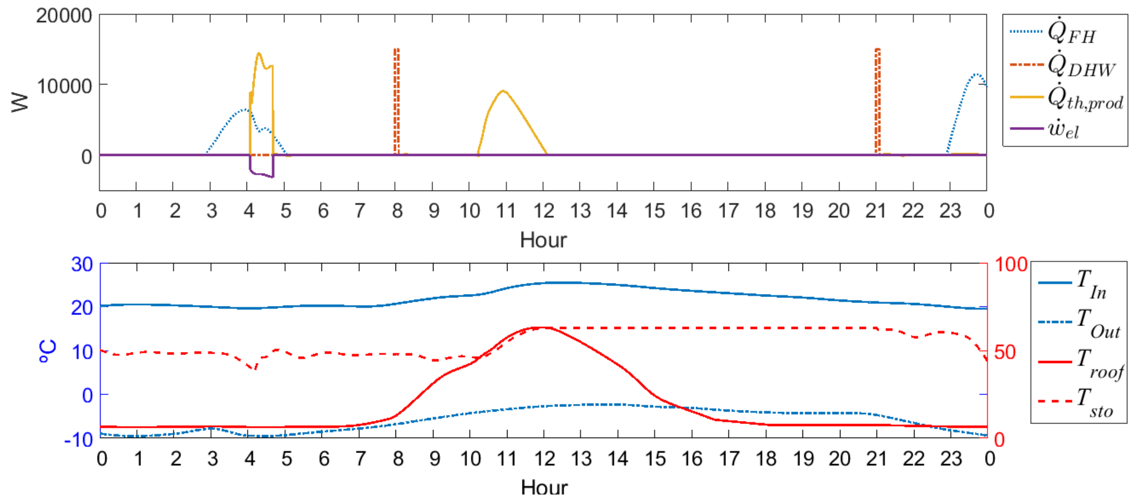


Figure 6. First, around midnight, the floor heating starts, decreasing the storage control temperature. Thus, the heat pump is activated following the same scheme as for the typical winter day. The difference is that around 10.30 a.m., the roof exhaust temperature is higher than the storage temperature and the system can therefore benefit from direct heating until 12 a.m. In that case, the direct heating allows to start the heat pump mode only once during day 62 to cover the heat demand of the building.

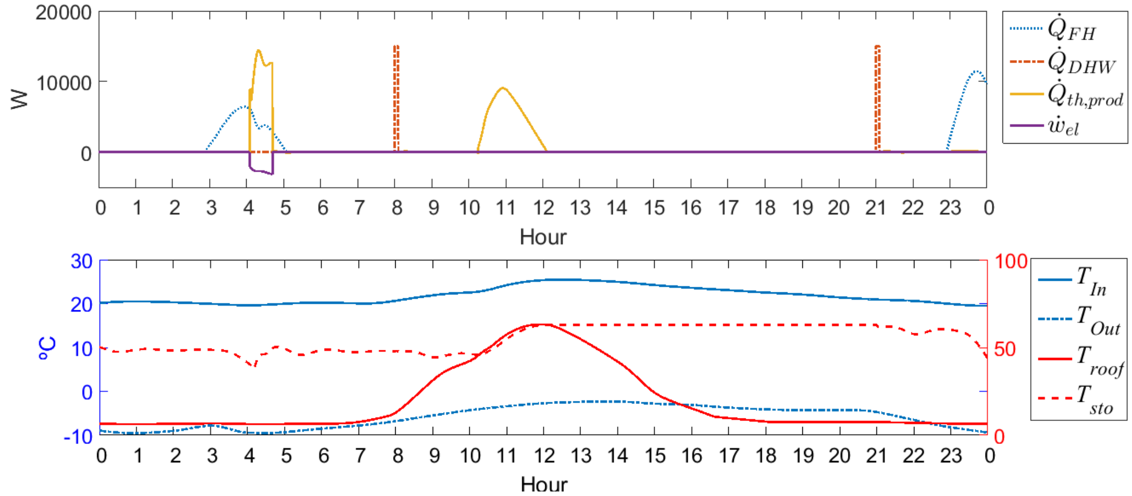


Figure 6: Dynamic simulation of the inversible unit coupled to a passive house for the 62nd day of the year.

### *3.3 Summer – Day 182*

Figure 7 presents the response of the inversible unit for a characteristic summer day for the study case in Denmark. Slightly before 8 a.m. the direct heating mode is activated since the roof temperature becomes higher than the storage temperature. When the storage temperature reaches its maximum value, the ORC mode can be activated to generate electricity. The electrical production of the ORC is low (compared to the nominal power, 5290 W) due to the high temperature of the water in the GHX. Since the heat demand is rather small (no floor heating, only DHW) and the capacity of the storage is hot enough there is no need to heat the thermal energy store. The ORC mode is therefore activated as long as the electrical production is greater than zero.

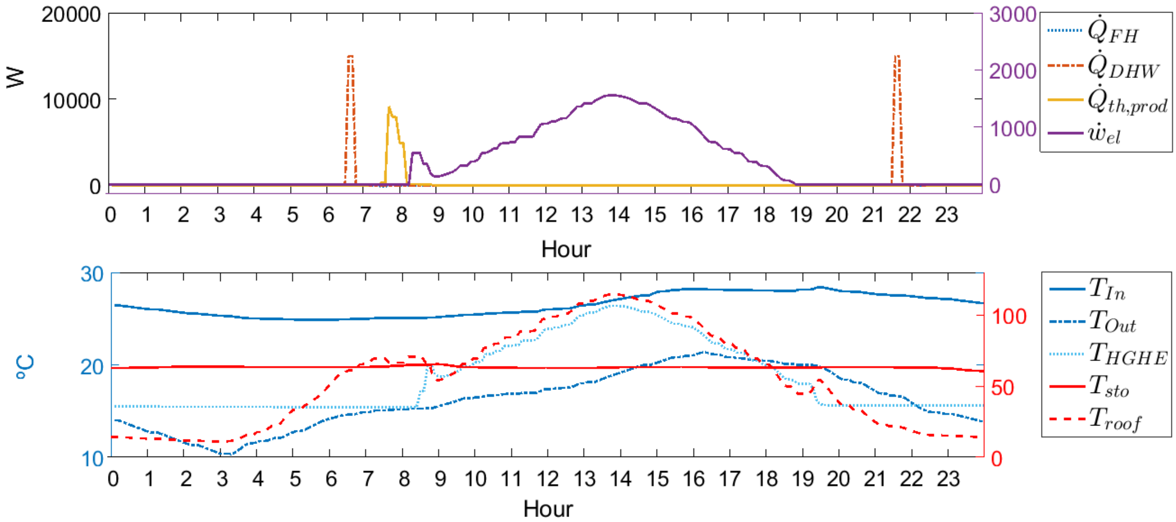


Figure 7: Dynamic simulation of the inversible unit coupled to a passive house for the 182nd day of the year. Mode 1 is ORC, mode 2 is direct heating and mode 3 is heat pump.

## 4. Annual performance

Yearly simulations are performed and evaluated through performance criteria:

- Gross electrical production [Wh]: the energy produced by the ORC (or the PV panels if specified) ($W_{el,prod}$).
- HP electrical consumption [Wh]: the electrical consumption of the HP ($W_{el,HP}$).
- Gross electrical consumption [Wh]: the sum of appliances, lighting and HP electrical consumption.
- Net electrical production [Wh]: the gross electrical production minus the gross electrical consumption ($W_{el,net}$).
- The total energy production of the unit [Wh] ($Q_{th,prod}$).
- DH energy [Wh]: the total thermal energy gained by means of the direct heating mode ($Q_{DH}$).
- B, Benefits [€]: the income benefits evaluated following Danish law (Equation (3)). It does not take any investment into account. $\dot{W}_{HP}$ is the electrical power consumption of the heat pump. $\dot{W}_{net}$ is the net electrical power, i.e. the electrical production minus the electrical power consumption of lighting and appliances. $P_r$ ~ 0.28 €.$W^{-1}$.$h^{-1}$ is the retail price considered when the net electrical power is negative, $P_{r,HP}$ is the retail price for the heat pump only ~ 0.22 €.$W^{-1}$.$h^{-1}$ and $P_{bb}$ is the buy-back tariff ~ 0.17 €.$W^{-1}$.$h^{-1}$ considered when the net electrical power ($\dot{W}_{net}$) is positive. Retail and buy-back tariffs are provided by real data from Denmark (Energinet 2015).

$$\text{If } \dot{W}_{net} > 0 \text{ then } B = \int_0^t \left(P_{\text{bb}}\,(\dot{W}_{net}) - P_{r,HP}.\dot{W}_{HP}\right).dt \qquad 4$$

$$\text{else } B = \int_0^t \left(P_{\text{r}}\,(\dot{W}_{net}) - P_{r,HP}.\dot{W}_{HP}\right).dt$$

- Supply cover factor or self-production rate ($\gamma_S$), which represents the fraction of energy produced by the ORC (or PV) which is used to cover instantaneous electrical consumption (Equation (4)) (Baetens et al., 2012).

$$\gamma_S = \frac{\sum \min\,(W_{cons.}, W_{prod})}{\sum W_{prod}} \qquad 5$$

- Demand cover factor or self-consumption rate ($\gamma_d$), which represents the fraction of energy consumption which has been produced by the ORC (or PV) (Equation (5)).

$$\gamma_D = \frac{\sum \min\,(W_{cons.}, W_{prod})}{\sum W_{cons.}} \qquad 6$$

For all the simulations in this paper, the set-points temperature of the storage, the set-point in the main room of the building and the solar roof are the same.

### *4.1 Reference case*

First, before establishing a sensivity analysis, a basic case yearly simulation corresponding to the real conditions of the house located in Herning, Denmark, is performed. In this simulation, there is one thermal storage of 500 liters for DHW and floor heating. Figure 8 presents a comparison of the electrical ORC production, heat pump electrical consumption and thermal energy provided by the direct heating mode for each month of the year. The heat pump is running during 5 months of the year, mainly in winter, leading to a total electricity consumption of 827 kWhe and heat supply of 3082 kWhth. Direct heating is used ten months of the year and produces 1207 kWth, representing 28.1 % of the total heat demand of the building during a year.

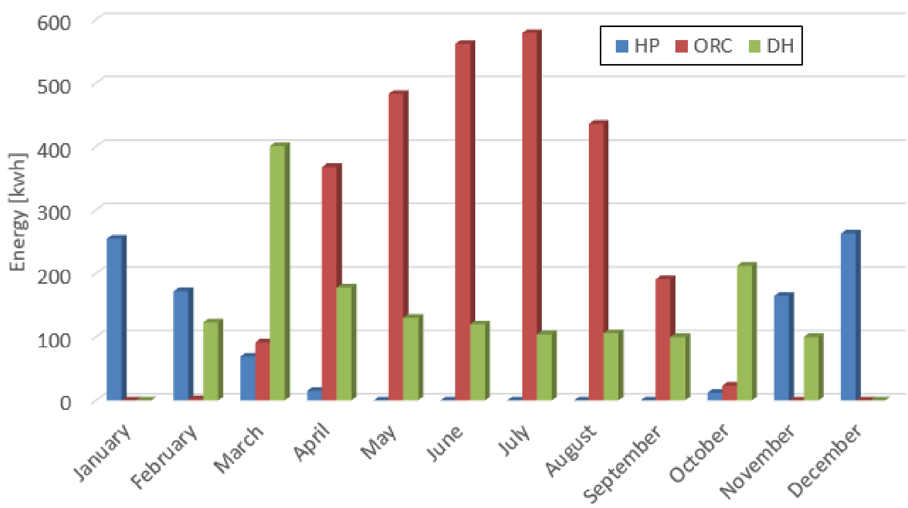


Figure 8: Comparison of the heat pump electrical consumption, electrical ORC production and thermal energy provided by the direct heating mode for each month of the year in the reference case.

The direct heating mode is less used in summer months compared to March and October because the heat demand for floor heating is significantly lower. The gross electrical ORC production is equal to 3012 kWhe, the lighting and appliances consumption reaches 1491 kWhe, leading to a net electrical production of 694 kWhe on a yearly basis. This demonstrates the ability of the current technology to get a Positive Energy Building in terms of electricity use. Using Equation (3), the annual running costs of the system in aforementioned conditions are 119€.

### *4.2 Results of the sensitivity analysis on the performance of the HP/ORC system*

After considering the basic case, it is interesting to compare the system behavior resulting from different climates. A former project (Knight et al. 2010) has shown that European climate can be divided into 5 different typical zones. The system is therefore simulated for 5 cities located in each zone (from north to south): Copenhagen, Frankfurt, Torino, Rome and Palermo. For comparison purposes the feed-in tariffs for the different locations was maintained as in the Danish case.

Secondly, two additional different building envelope characteristics –K15 and K30 (Masy et al., 2015) are studied in all climates. They differ in terms of coefficient of heat transmission and air tightness (see appendices - Table A3 annexes). Finally – as proposed in Georges et al. 2013 -two additional Light and Appliances profiles (L&A) are simulated with the reference Danish building characteristics. The latter differ in the magnitude of power demand. In decreasing order of magnitude L&A 2010 (3000 kWh/year) is characterized by highest demand, followed by L&A 2030 (2000 kWh/ year) and L&A Danish (1491kWh/year). Table 2 shows the results of sensitivity analysis on the performance of the HP/ORC system under different conditions of climate, insulation and lights and appliances demand according to the performance parameters listed in chapter Annual performance.

Table 2: Results of the sensitivity analysis. ($Q_{th,prod}$ is the toal energy production of the HP/ORC unit, $W_{el,prod}$ is the gross electrical production, $W_{el,HP}$ is the HP electrical consumption, $W_{el,net}$ is the net electrical production). $B$ are the income benefits, $\gamma_S$ is the self-production rate, $\gamma_d$ is the self-consumption rate, $Q_{DH}$ is the DH energy).

| Building | L&A | Location | $Q_{th,prod}$ [kWh] | $W_{el,prod}$ [kWh] | $W_{el,hp}$ [kWh] | $W_{net}$ [kWh] | Benefits [€] | $\gamma_s$ | $\gamma_D$ | $Q_{dh}$ [kWh] |
|---|---|---|---|---|---|---|---|---|---|---|
| *Danish* | 2010 | Copenhagen | 3597 | 3015 | 690 | -675 | -501 | 0,13 | 0,13 | 1057 |
| | | Frankfurt | 3291 | 3609 | 572 | 37 | -368 | 0,119 | 0,14 | 1180 |
| | | Torino | 2243 | 5379 | 189 | 2190 | 38 | 0,1 | 0,18 | 1523 |
| | | Roma | 1072 | 6646 | 16 | 3630 | 312 | 0,1 | 0,23 | 990 |
| | | Palermo | 861 | 8597 | 0 | 5597 | 666 | 0,096 | 0,27 | 845 |
| | Danish | Copenhagen | 4289 | 3012 | 827 | 694 | -119 | 0,071 | 0,138 | 1207 |
| | | Frankfurt | 3879 | 3607 | 699 | 1417 | 15 | 0,065 | 0,15 | 1292 |
| | | Torino | 2700 | 5371 | 251 | 3629 | 422 | 0,054 | 0,185 | 1726 |
| | | Roma | 1301 | 6639 | 35 | 5113 | 695 | 0,053 | 0,226 | 1148 |
| | | Palermo | 889 | 8597 | 0 | 7106 | 1046 | 0,049 | 0,27 | 872 |
| | 2030 | Copenhagen | 4025 | 3014 | 783 | 231 | -260 | 0,093 | 0,133 | 1134 |
| | | Frankfurt | 3652 | 3609 | 647 | 962 | -125 | 0,084 | 0,145 | 1254 |
| | | Torino | 2545 | 5374 | 226 | 3148 | 281 | 0,071 | 0,181 | 1671 |
| | | Roma | 1211 | 6643 | 26 | 4617 | 553 | 0,07 | 0,22 | 1088 |
| | | Palermo | 875 | 8596 | 0 | 6596 | 904 | 0,065 | 0,26 | 859 |
| *K15* | Danish | Copenhagen | 2887 | 3021 | 535 | 995 | -38 | 0,047 | 0,096 | 912 |
| | | Frankfurt | 2685 | 3615 | 447 | 1677 | 81 | 0,042 | 0,1 | 1034 |
| | | Torino | 1772 | 5386 | 120 | 3775 | 464 | 0,036 | 0,131 | 1304 |
| | | Roma | 980 | 6648 | 12 | 5145 | 708 | 0,036 | 0,159 | 917 |
| | | Palermo | 863 | 8596 | 0 | 7105 | 1048 | 0,033 | 0,19 | 847 |
| *K30* | Danish | Copenhagen | 8667 | 2987 | 1723 | -227 | -318 | 0,046 | 0,092 | 2031 |
| | | Frankfurt | 7804 | 3573 | 1457 | 625 | -156 | 0,041 | 0,098 | 2206 |
| | | Torino | 5956 | 5334 | 803 | 3040 | 300 | 0,035 | 0,128 | 2837 |
| | | Roma | 3254 | 6585 | 196 | 4898 | 655 | 0,035 | 0,155 | 2468 |
| | | Palermo | 1670 | 8562 | 15 | 7056 | 1038 | 0,032 | 0,187 | 1586 |

From Table 2, it can be concluded that for any building and light and appliances demand sunniest locations (south Europe) yields to higher power production and thus, higher financial benefits. On the other hand, the heat pump is almost never used in southern locations, because the heat demand is small and, therefore can benefit from the direct heating. On the contrary, northernmost locations present low heat energy provided by direct heating. There is an optimal location in latitude close to Torino that shows the best compromise to benefit optimally of the thermal energy from the DH. It is interesting to note that an increase of lights and appliances demand - in all locations - decreases the net power output and benefits, but also decreases the heat pump power consumption. This is due to the internal heat gains by means of light and applicances,which decrease the heating demand. On the other hand, it is shown that lower levels of insulation lead to higher heating demand covered by DH without compromising the ORC power output and the finantial benefits.

### *4.3 Comparison with a heat pump combined with photovoltaic panels*

In a former article (Dumont et al, 2015b), a comparison is performed between the HP/ORC inversible unit and a classical mature solution for Positive Energy Buildings which is composed of photovoltaic panels combined with a water to water heat pump (HP/PV). Another alternative single-technology capable of delivering heat and electric power is PVT but it is considered out of the scope of this study( He et al, 2006, Herrando et al, 2014 and Dupeyrat et al, 2014). In this former paper (Dumont et al, 2015b), the area of photovoltaic panel is fixed in a way that the electrical peak power is the same as the HP/ORC inversible unit in typical summer conditions. The best system is always the HP/PV system in terms of electrical production, income benefits and matching of the production and consumption. Nevertheless, an interesting advantage of the inversible unit is the lower heat pump electrical consumption which makes this system more profitable if no electricity can be bought on the grid (isolated network for example). Furthermore, an economic feasibility study the total cost (income benefit and investment) of the HP/ORC system is compared to the cost of the HP/PV system. The inversible system is never profitable in the base case with a heat demand corresponding to the real house. But, if the heat demand is significantly higher (8 times higher DHW consumption) the inversible unit is much more profitable.

## 5. Conclusion

The recent interest for Positive Energy Buildings (PEB) has led to develop new technologies and solutions. In this paper, the inversible heat pump/organic Rankine cycle coupled to a passive house is studied. This technology is a promising way to achieve a PEB. The modelling of each submodel (ground heat exchanger, thermal energy storage, building, solar roof, inversible HP/ORC unit and the control) are described extensively. Simulations have shown that this technology leads to a PEB on a annual basis. Also, a sensitivity study has shown the following conclusions

- The HP/ORC system presents a positive net electrical production while covering the total heat demand of the building over a year, even in cold climates such as that of Denmark.
- The climate in southernmost cities is much more favorable for ORC because it works longer and closer to nominal conditions.
- There is an optimum location (latitudes around Torino) where the direct heating is maximum.
- A low insulation of the building and/or a low energy lighting and appliances profile leads to a better exploitation of the system profiting of more energy from direct heating.
- When compared to a heat pump coupled with PV panels, HP/ORC unit shows that the system could only be profitable in the case of a large heat demand of the building and/or restriction on buying electricity to the grid. More generally, this means that buildings with a high heat demand, everything else being constant, are profitable for the inversible unit. A tall building or a building with high DHW consumption could fit this constraint (office building, hospital, prison, stadium, etc.).

## References


Abdul-Zahra, A. and T. Fassnacht and A. Wagner. 2014. "Evaluation of the combination of hybrid photovoltaic solar thermal collectors with air to water heat pumps." doi:10.1016/j.apenergy.2014.01.061

Almeida, A. and P. Fonseca. 2007. "Residential monitoring to decrease energy use and carbon emissions in Europe." European council for energy efficient economy 2007, 1261-1271. http://remodece.isr.uc.pt/news/Paper_DeAlmeida.pdf

Baetens, R. De Coninck, R. Van Roy, J., Verbruggen, B. Driense, J. Helsen, L. Saelens, D. 2012 "Assessing electrical bottlenecks at feeder level for residential net zero-buildings by integrated system simulation", Applied Energy, vol. 96, pp. 74-83

Bircher, S, Skou, N. Jensen, K.H., Walker, J.P. and Rasmussen, L. 2012 "A soil moisture and temperature network for SMOS validation in Western DK", Hydrol.Earth Syst. Sci. 16, 1445-1463

Bouvenot, J-B., Siroux, M., Latour, B. and Flament, B. 2015. "Dwellings electrical and DHW load profiles generators development for µCHP systems using RES coupled to buildings applications." 6th International Building Physics Conference, IBPC 2015, Energy Procedia 00 (2015) 000–000.

Burhenne, S., D. Wystrcil, M. Elci, S. Narmsara and S. 2015. "Building performance simulation using modelica: analysis of the current state and application areas." Proceedings of BS2013: 13th Conference of International Building Performance Simulation Association, Chambéry, France, August 26-28.

Carmo, C., Dumont, O., Elmegaard, B., Nielsen, Detlefsen, "Experimental validation of a domestic stratified hot water tank model in Modelica for annual performance assessment"." ORC 2015 conference.

Danish energy agency, 2015. https://www.retsinformation.dk/forms/r0710.aspx?id=152758, accessed on the 22th of July 2015.

Duffie, J. A. and W. A. Beckham. 2006. "Solar thermal engineering of thermal processes."John wiley and sons, ISBN: 978-0-470-87366-3.

Dumont, O., Quoilin, S., Lemort, V., 2014a. Experimental investigation of a scroll unit used as a compressor and as an expander in a reversible Heat Pump/ORC unit. Proceedings of the refrigeration conference in Purdue.

Dumont, O., C. Carmo, F. Randaxhe, S. Quoilin and V. Lemort. 2014b. "Simulation of a passive house coupled with a heat pump/organic Rankine cycle reversible unit." Proceedings of the 9th International Conference on System Simulation in Buildings (SSB2014).

Dumont, O., Quoilin, S., Lemort, V., 2015a. "Experimental investigation of a reversible heat pump / organic Rankine cycle unit designed to be coupled with a passive house (Net Zero Energy Building)", International Journal of Refrigeration, http://dx.doi.org/10.1016/j.ijrefrig.2015.03.008.

Dumont, O., Carmo, C., Randaxhe, F., Quoilin, S., Lemort, V., 2015b. "Performance comparison of two types of technologies associated with a positive energy building: a reversible heat pump/ORC unit and a heat pump coupled with PV panels". Proceedings of the ISES Solar World Congress (SWC 2015). International Solar Energy Society, ISES, 2015. p. 1-6.

Dupeyrat P., Ménézo, P., Fortuin S., 2014. "Study of the thermal and electrical performances of PVT solar hot water system." Energy and Buildings 68, 751-755.

Energinet. 2015. http://energinet.dk/DA/El/Solceller/Har-du-solceller/Sider/Pristillaeg.aspx, accessed th 2st of January 2015.

European Comission. 2011. Market observatory for energy, https://ec.europa.eu/energy/sites/ener/files/documents/quarterly-gas_q3_2014_final_0.pdf.

EnergyPlus, 2015. http://apps1.eere.energy.gov/buildings/energyplus/weatherdata_about.cfm, accessed the 18th of May 2015.

EV-power, 2014. http://www.ev-power.eu/Winston-300Ah-1000Ah/, accessed the 29th of october 2014.

Fischer, S.,Heidemann W., Müller-Steinhagen, H., Perers, B., , Bergquist, P., Hellströmd, B., 2004. “Collector test method under quasi-dynamic conditions according to the European Standard EN 12975-2”, Solar Energy 76, 117-123.

Freeman, J., Hellgardt, K., Markides, C. 2015. “An assessment of solar-powered organic Rankine cycle systems for combined heating and power in UK domestic applications”, Applied Energy 138, 605-620.

Georges, E., S. Gendebien, S. Bertagnolio, and V. Lemort. 2013a. “Modeling and simulation of the domestic energy use in Belgium.” *Proceedings of CLIMA 2013 11th REHVA World Congress & 8th International Conference on IAQVEC*.

Georges, E., S. Gendebien, S. Bertagnolio, and V. Lemort. 2013 b. “ Impact of the integration of various heating technologies on the energy load profiles of the Belgian residential building stock”, Proceedings of the 8th Renewable Energy Storage Conference and Exhibition (IRES 2013)Innogie ApS. 2013. “Thermal solar absorber system generating heat and electricity.” United States Patent Application Publication, US 2013/025778 A1, https://patentscope.wipo.int/search/en/detail.jsf?docId=WO2012041323&recNum=27&docAn=DK2011050363&queryString=(FP/solar%20AND%20FP/thermal%20AND%20FP/electricity)%20&maxRec=107.

He, W., Chow, T., Jianping, Lu, J., Pei, G., Chan. G., 2006. “Hybrid photovoltaic and thermal solar-collector designed for natural circulation of water.” Applied Energy 83, 199-210.

Herrando, M., Markides, C., Hellgardt, K., 2014. “A UK-based assessment of hybrid PV and solar-thermal systems for domestic heating and power: System performance.” Applied Energy 122, 288-309.

Kalaiselvam, S., and R. Parameshwaran. 2014. “Thermal Energy Storage Technologies for Sustainability: Systems Design, Assessment and Applications.” Academic Press, Boston, Pages i-ii, ISBN 780124172913, http://dx.doi.org/10.1016/B978-0-12-417291-3.09983-7.

Klein, S. A. 1975. “Calculation of flat-plate loss coefficient.” Solar Energy, 17, 79. http://adsabs.harvard.edu/abs/1975SoEn...17...79K.

Knight I., J. Adnot J., J-L. Alexandre, P. Andre., M-N. Assimakopoulos, V. Butala, R. Hitchin, M. Masoero, C. Spitzbart and D. Wright. 2010. “HARMONAC - Harmonizing Air Conditioning Inspection and Audit, procedures in the Tertiary Building Sector, energy Consumption in European Air Conditioning Systems and the Air”, https://ec.europa.eu/energy/intelligent/projects/en/projects/harmonac.

Kost, C., J. Mayer, J. Thomsen, N. Hartmann, C. Senkpiel, S. Philipps, S. Nold, S. Lude, N. Saad, and T. Schlegl. 2013. ”Levelized cost of electricity renewable energy technologies.” Fraunhofer ISE, https://www.ise.fraunhofer.de/en/publications/veroeffentlichungen-pdf-dateien-en/studien-und-konzeptpapiere/study-levelized-cost-of-electricity-renewable-energies.pdf

Lund, H., A. Marszal, and P. Heiselber. 2011. “Zero energy buildings and mismatch compensation factors.” Energy and buildings, 43, 7, 1646-1654, doi:10.1016/j.enbuild.2011.03.006.

Masy, G. 2007. Definition and validation of a simplified multizone dynamic building moçdel connected to heating system and HVAC unit. PhD thesis. Liege.

Masy, G., E. Georges, C. Verhelst, V. Lemort and P. André. 2015. “Smart Grid Energy Flexible Buildings through the use of Heat Pumps and Building Thermal Mass as Energy Storage in the Belgian context.” *Science and Technology for the Built Environment – Ashrae, DOI:10.1080/23744731.2015.1035590.*

Marszal, A. J., P. Heiselberg, J. S., Bourrelle, E. Musall, K. Voss, I. Sartori and A. Napolitano. 2011. “Zero Energy Building – A review of definitions and calculation methodologies.”, Energy and Buildings, Volume 43, Issue 4, Pages 971-979, ISSN 0378-7788, Zero Energy Building – A review of definitions and calculation methodologies.

Muller, D. And A. H. Badakhshani. 2010. ”Gebaude und Anlagensimulati mit modelica.” Proceedings of BauSIM 2010, http://info.tuwien.ac.at/bausim/conftool/mueller-2010-gekoppelte_gebaeude-_und_anlagensimulation_mit_modelica-198.pdf.

Nytsch-Geusen, M. And S. Unger. 2009. ”Modelling of complex thermal energy supply systems based on the modelica-library fluidflow.” Proceedings 6th International Modelica Conference, http://webcache.googleusercontent.com/search?q=cache:D2BJ4wVYr8IJ:citeseerx.ist.psu.edu/viewdoc/summary%3Fdoi%3D10.1.1.472.1996+&cd=3&hl=fr&ct=clnk&gl=be.

Perers, B. 1997. “An improved dynamic solar collector test method for determination of non-linear optical and thermal characteristics with multiple regression.” Solar Energy, Volume 59, 163-178.

PICIR (Potsdam Institute for Climate Impact Research), 2015. www.pik-potsdam.de., accessed on the 30th of July.

Quoilin, S., O. Dumont and V. Lemort. 2013. “Design, modelling and performance optimization of a reversible HP/ORC prototype.”  Proceedings of the ORC 2013 conference.

Quoilin S., A. Desideri, J. Wronski and I. Bell. 2014. “ThermoCycle: A Modelica library for the simulation of thermodynamic systems.” Proceedings of the 10th International Modelica Conference 2014.

Quoilin, S., O. Dumont, K. Harley, V. Lemort. 2015. “Design, modeling and performance optimization of a reversible Heat Pump / Organic Rankine Cycle prototype.” Journal of Engineering for Gas Turbines and Power, doi:10.1115/1.4031004

Schimpf, S., K. Uitz,  and R. Span. 2011. “Simulation of a solar assisted combined heat pump-organic Rankine cycle system.” Proceedings of World renewable Energy Congress 2011 Sweden.

Schnieders, J. 1997. “Comparison of the energy yield predictions of stationary and dynamic solar collector models and the models' accuracy in the description of a vacuum tube collector”, Solar Energy 61, 179-190.

TESS, 2006. “Standard component library overview.” http://web.mit.edu/parmstr/Public/Documentation/03-ComponentLibraryOverview.pdf

Chow, T. 2003. “Performance analysis of photovoltaic-thermal collector by explicit dynamic model”, Solar Energy 75, 2003, 143-152.

Trnsys, 2015. “TESS COMPONENT LIBRARIES.” http://www.trnsys.com/tess-libraries/TESSLibs17_General_Descriptions.pdf, accessed the 1st of September 2015.
Wetter, M., W. Zuo, and T. S. Nouidui, 2011. “Recent Developments of the Modelica “Buildings, Library for Building Energy and Control Systems.” Proceedings of the 8th International Modelica Conference.
Wetter, M., W. Zou, T. S Nouidui and X. Pang. 2013. “Modelica Buildings library.” Journal of Building Performance Simulation, March 2013, DOI:10.1080/19401493.2013.765506.
Wang, P.G., M. Scharling, K. P. Nielsen and C. Kern-Hansen, C. 2010. ”Technical Report 13-19: 2001 – 2010 Danish Design Reference Year, Climate Dataset for Technical Dimensioning in Building, construction and other Sectors.” http://www.dmi.dk/fileadmin/Rapporter/TR/tr13-19.pdf

## Appendices

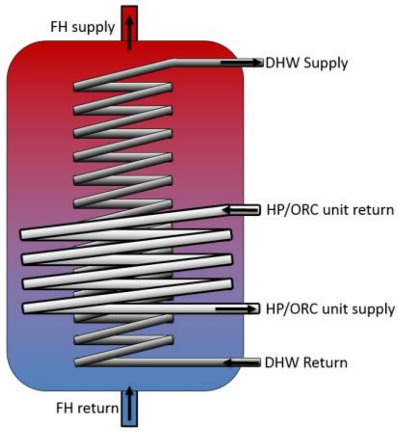


Figure A1: Hydraulic scheme of the thermal heat storage. Unit loop is the reversible HP/ORC unit. In heat pump mode, it is connected to the condenser and in direct heating mode is is connected to the solar roof.

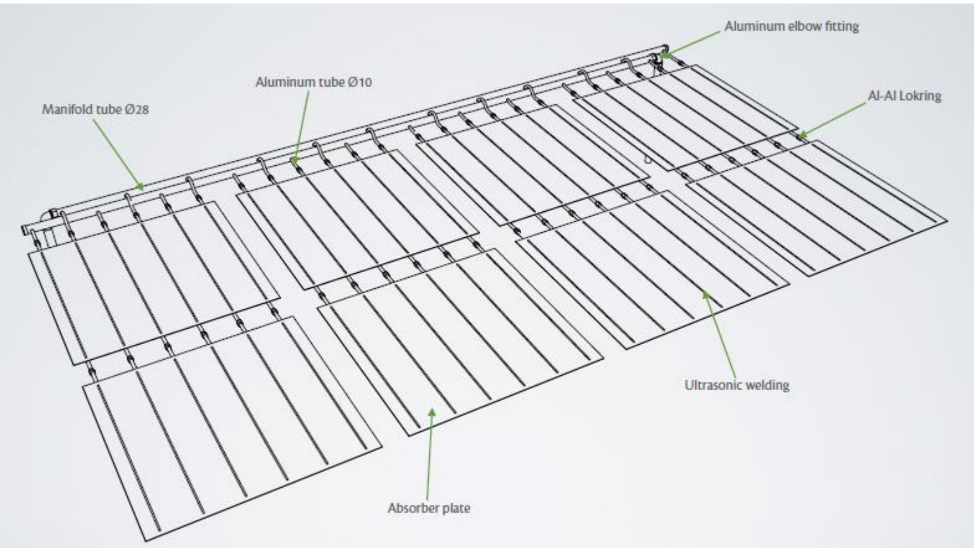


Figure A2: Solar roof scheme

Table A1: Terms of Equation (**Erreur ! Source du renvoi introuvable.**)

| Term | Name | Value/expression |
|---|---|---|
| β | Collector tilt | 5 [°C] |
| v | Empirical constant | $520(1-0.000051\beta^2)$ |
| e | Empirical variable | $0.43(1-\frac{100}{T_m})$ |
| $\varepsilon_g$ | Emitence of glass | 0.88 |
| $\varepsilon_p$ | Emitence of plate | 0.95 |
| n | Empirical constant | $(1+0.089.h_w-0.1166h_w\varepsilon_p)(1+0.07866N)$ |
| $h_w$ | Wind heat transfer coefficient | 2 [$W.m^{-2}.K^{-1}$] |
| s | Empirical constant | 0.00591 |
| z | Empirical constant | 0.133 |

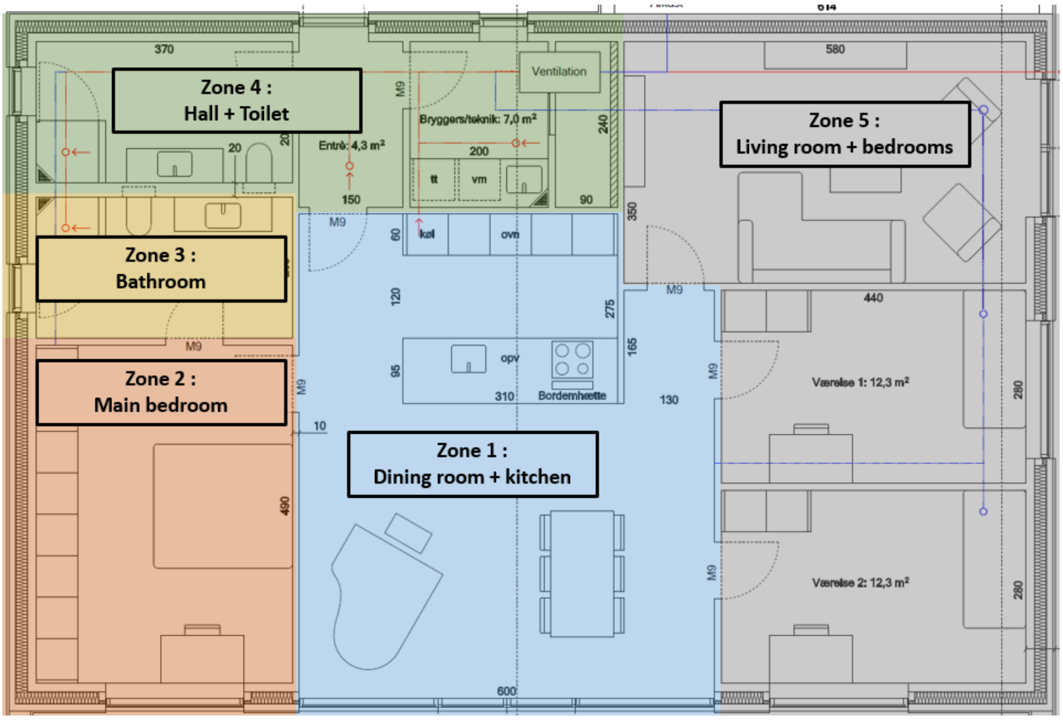


Figure A3: Division of the house into 5 zones.

Table A2: 5 zones of the house characteristics

| | **Unit** | **Zone 1** | **Zone 2** | **Zone 3** | **Zone 4** | **Zone 5** |
|---|---|---|---|---|---|---|
| Floor area | m² | 41.8 | 18.2 | 7.8 | 19.1 | 45.7 |
| Volume | m³ | 117.2 | 45.5 | 19.5 | 47.8 | 114.3 |
| Slab U-Value | W/m².K | 0.08 | 0.08 | 0.08 | 0.08 | 0.08 |
| Roof U-Value | W/m².K | 0.09 | 0.09 | 0.09 | 0.09 | 0.09 |
| External wall area | m² | none | 20.4 | 4.5 | 24.8 | 41.5 |
| External wall U-value | W/m².K | none | 0.15 | 0.15 | 0.15 | 0.15 |
| Window area (orientation) | m² | 14.7(S) | 2.4(S) | 0.84(W) | 0.84(W) 0.84(N) | 6.7(E) 2.4(S) |
| Window U-value | W/m².K | 0.63 | 0.68 | 0.8 | 0.8 | 0.8 |
| Window solar factor | - | 0.5 | 0.5 | 0.5 | 0.5 | 0.5 |
| Infiltration rate | ACH | 0.3 | 0.3 | 0.3 | 0.3 | 0.3 |
| Space activity | - | Kitchen Dining | Main Bedroom | Bathroom | Hall Others | Living Bedroom |
| Lighting nominal power | W/m² | 5 | 5 | 3 | 3 | 5 |
| Appliances nominal power | W/m² | 3 | 3 | 3 | 3 | 3 |
| Air temperature Setpoint | °C | 20 | Only imposed in zone 1 | Only imposed in zone 1 | Only imposed in zone 1 | Only imposed in zone 1 |

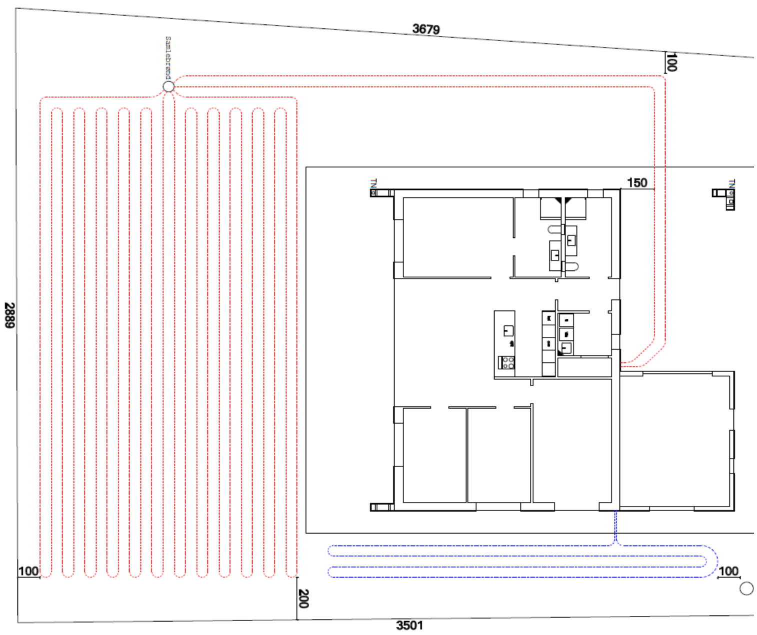


Figure A4: Layout of the GHX. Black line is the building, blue line is a cooling system and red lines are the GHX with two main hoses of connection.

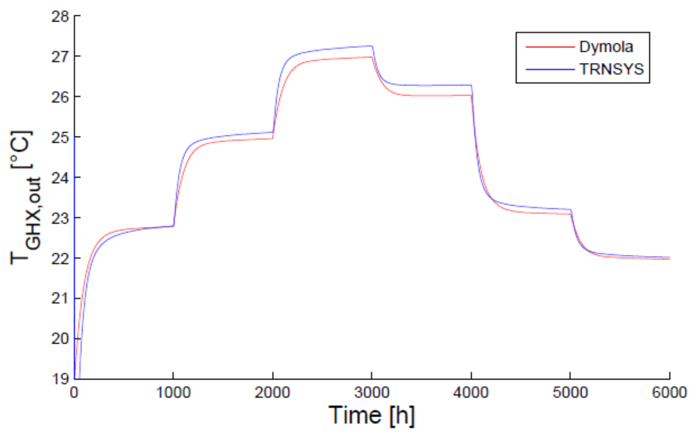


Figure A5: Water outlet temperature of the ground heat exchanger submitted to steps: Finite element model versus reduced order model.  A maximum deviation of 0.5 K is observed for the prediction of the water outlet temperature. The values of the calibrated parameters are given in Figue A7.

| | Parameter | Value | Unit |
|---|---|---|---|
| Surface | Thermal Capacity | $3E07$ | $J/K$ |
| | Related thickness | 0.033 | $m$ |
| | Thermal resistance | 0.0011 | $K/W$ |
| | Convective resistance | $1.58E-04$ | $K/W$ |
| Subsoil | Thermal Capacity | $4E09$ | $J/K$ |
| | Related thickness | 4.47 | $m$ |
| | Thermal resistance | 0.005 | $K/W$ |
| Central soil | Thermal Capacity | $1.2E09$ | $J/K$ |
| | Related thickness | 2.01 | $m$ |
| Pipes | Convective resistance | $1.26E-04$ | $K/W$ |
| | Tube resistance | $4.89E-05$ | $K/W$ |
| | Soil resistance | $2E-04$ | $K/W$ |
| Contact surface | Area | 299 | $m^2$ |

Figure A6: Validated parameters of the reduced order model

Table A3: Envelope characteristics of different typical buildings

| Coefficient of heat transmission | Danish | K15 | K30 |
|---|---|---|---|
| Roof [$W.m^{-2}.K^{-1}$] | 0.09 | 0.093 | 0.228 |
| Floor slab [$W.m^{-2}.K^{-1}$] | 0.08 | 0.123 | 0.258 |
| External wall [$W.m^{-2}.K^{-1}$] | 0.15 | 0.102 | 0.245 |
| Window [$W.m^{-2}.K^{-1}$] | 0.63 | 0.9 | 1.2 |
| Infiltration rate (50 Pa) [$m^3.h^{-1}.m^{-2}$] | 2.51 | 0.6 | 0.35 |